Direct Measurement of Shear-Induced Cross-Correlations of Brownian Motion

A. Ziehl,[1] J. Bammert,[2] L. Holzer,[2] C. Wagner,[1] and W. Zimmermann[2]

[1]*Technische Physik, Universität des Saarlandes, 66041 Saarbrücken, Germany*
[2]*Theoretische Physik I, Universität Bayreuth, 95440 Bayreuth, Germany*
(Received 26 July 2009; published 3 December 2009)

Shear-induced cross-correlations of particle fluctuations perpendicular and along streamlines are investigated experimentally and theoretically. Direct measurements of the Brownian motion of micron-sized beads, held by optical tweezers in a shear-flow cell, show a strong time asymmetry in the cross-correlation, which is caused by the non-normal amplification of fluctuations. Complementary measurements on the single particle probability distribution substantiate this behavior and both results are consistent with a Langevin model. In addition, a shear-induced anticorrelation between orthogonal random displacements of two trapped and hydrodynamically interacting particles is detected, having one or two extrema in time, depending on the positions of the particles.

The Brownian motion of particles in fluids and their hydrodynamic interactions are of central importance in chemical and biological physics as well as in material science and engineering [1–4]. However, our understanding of the dynamics of particles in flows is still far from complete. Direct observations of particles at the mesoscale substantially contribute to our understanding of their dynamics. At this scale optical tweezers are a powerful experimental technique [5] with a number of innovative applications. They include the detection of anticorrelations between hydrodynamically interacting Brownian particles [6], propagation of hydrodynamic interactions [7], short-time inertial response of viscoelastic fluids [8], two-point microrheology [9], anomalous vibrational dispersion [10], and particle sorting techniques [11].

Neutral colloidal particles moving relatively to each other interact via the fluid and these hydrodynamic interactions decay with the particle distance [2]. In shear flow little is known about the dynamics of Brownian particle motion and the hydrodynamic interaction effects in spite of their fundamental relevance and importance in applications in microfluidics, Taylor dispersion [12], and in fluid mixing [4,13]. In time dependent fields and in shear flow surprising deterministic particle dynamics may be induced by hydrodynamic interactions [14]. For polymers it is the interplay of shear flow and fluctuations which leads already at low Reynolds numbers, to rich dynamics [15], the so-called molecular individualism [16], causing elastic turbulence even in diluted polymer solutions [17] and spectacular mixing behavior [13].

It is the contribution $(\mathbf{u} \cdot \nabla)\mathbf{u}$ to the Navier-Stokes equation which causes interesting transient phenomena in shear flows near the onset of turbulence [18], as well as amplifications of fluctuations and their cross-correlations along and perpendicular to straight streamlines [19,20]. A cross-correlation is also expected between orthogonal particle-fluctuations in the shear plane, because random jumps of a particle between neighboring streamlines of

different velocity lead to a change of the particle's velocity and displacement along the streamlines, similar as via fluctuations. In some parameter ranges, inertia effects may become important [21–23]. Cross-correlations between perpendicular fluid-velocity fluctuations and perpendicular fluctuations of particles are expected to be strongly asymmetric in time [19,23,24]. In dynamic light-scattering experiments certain aspects of these shear-induced cross-correlations were observed indirectly [25], but a direct measurement and characterization of related particle fluctuations is missing.

Here we investigate in a linear shear flow the fluctuations of a single particle in a potential minimum and of two hydrodynamically interacting particles trapped by two neighboring potentials. We use a special shear-flow cell, where one or two micron-sized beads are held at its center by optical tweezers. The time asymmetry of shear-induced cross-correlations were determined directly by measuring the particle's positional fluctuations. In addition the probability distribution of a single particle in a trap was measured, which can be also calculated in terms of a Langevin model, similar to the correlations. Both the probability distribution and the correlation can be fitted by using the same value of the shear rate, which altogether gives a consistent picture of not yet directly observed shear-induced cross-correlations of particle fluctuations.

By a dual beam optical tweezer setup, composed of two solid state lasers and an oil immersion objective with a numerical aperture of 1.4, two harmonic potentials are generated in an inverted microscope (Nikon TE 2000-S) to capture uncharged polystyrene beads (Duke Scientific Corporation, R0300) with a diameter of 3 μm in a flow of distilled water. The beads were observed with a high speed camera (IDT, X-Stream, XS-5) of 15 kHz and their positions were determined with a correlation tracking algorithm with a spatial resolution of ± 4 nm [26]. To avoid any interference of the two potentials at small distances and to maximize the hydrodynamic interaction effect between the

two particles, they where held at a distance of $d = 4 \ \mu$m. In a microfluidic device with two counter flows, as shown in Fig. 1, a linear shear gradient with a vanishing mean velocity was generated at the center of the cell, as experimentally verified by micro-PIV (see inset in Fig. 1). The design of the flow chamber was optimized by numerical simulations of the incompressible Navier-Stokes equation (Multiphysics 3.4, Comsol AB, Stockholm, Sweden). The small width in x direction of the center piece of the chamber was chosen in order to minimize flow in y direction. The curved form of the boundaries was found to suppress vortices. The channel was manufactured by standard soft lithographic techniques and the flow was driven by gravitational potential difference. The distance of the beads from the wall was always larger than 10 μm in the z direction and 25 μm in the xy plane. Hence boundary effects on the bead fluctuations could be excluded within our experimental resolution, as verified by measurements without flow, which were in very good agreement with previous results (see, e.g., Ref. [6]). However, with flow the experimental noise becomes larger, especially at longer correlation times. The value of the shear rate $\dot\gamma$ has been extracted from the fits of the correlation data and by particle tracking methods. The highest shear rate that did not lead to an escape of the particles from the traps was $\dot\gamma \simeq 50 \text{ s}^{-1}$ [27].

One or two Brownian particles with coordinates $\mathbf{r}_i = (x_i, y_i, z_i)$ ($i = 1, 2$) are held in a linear shear flow $\mathbf{u}(y_i) = \dot\gamma y_i \hat{\mathbf{e}}_x$ by forces $\mathbf{f}_i^V = k(\mathbf{p}_i - \mathbf{r}_i)$ close to the minima $\mathbf{p}_i$ of two harmonic potentials $V_i = \frac{k}{2}(\mathbf{p}_i - \mathbf{r}_i)^2$ (spring constant k). The overdamped particle motion is described by a Langevin equation [2]:

$$\dot{\mathbf{r}}_i = \mathbf{u}(\mathbf{r}_i) + \mathsf{H}_{ij}(\mathbf{f}_j^V + \mathbf{f}_j^S). \qquad (1)$$

The mobility matrix H_{ij} accounts for the Stokes friction and the hydrodynamic interactions between them. Here we
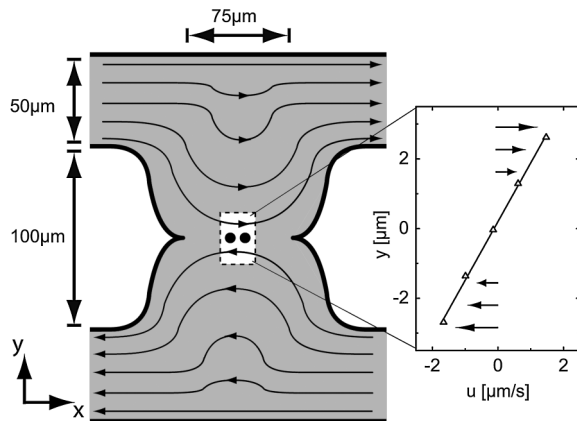

FIG. 1. A cell cross section (lithographic mask) is shown with 150 μm depth in the z direction having opposite flow directions in its upper and lower channel and a linear shear profile at its center: see inset with PIV data (Δ) and linear fit. One or two particles at a distance $d = 4 \ \mu$m were held by optical tweezers in the center of the linear velocity profile $\mathbf{u}(y)$.

use the Oseen approximation

$$\mathsf{H}_{11} = \mathsf{H}_{22} = \frac{1}{\zeta}\mathsf{E}, \qquad (2)$$

$$\mathsf{H}_{12} = \mathsf{H}_{21} = \frac{1}{\zeta}\frac{3a}{4r_{12}}\left[\mathsf{E} + \frac{\mathbf{r}_{12}\mathbf{r}_{12}^T}{r_{12}^2}\right], \qquad (3)$$

with the Stokes friction coefficient $\zeta = 6\pi\eta a$ of a point particle of effective hydrodynamic radius a in a fluid of viscosity η and the unity matrix E. $\mathbf{r}_{12} = \mathbf{r}_1 - \mathbf{r}_2$ is the bead distance and r_{12} is its norm, $\tau = \zeta/k$ the particle relaxation time in the potential and $W = \dot\gamma\tau$ the Weissenberg number. The Brownian particle motion is driven by the stochastic forces $\mathbf{f}_i^S(t)$ in Eq. (1), for which we assume vanishing mean values and correlation times:

$$\langle\mathbf{f}_i^S(t)\rangle = 0, \qquad (4)$$

$$\langle\mathbf{f}_i^S(t)\mathbf{f}_j^S(t')\rangle = 2k_BT\mathsf{H}_{ij}^{-1}\delta(t - t'). \qquad (5)$$

At first we investigate the Brownian motion of a single trapped particle in shear flow. Its autocorrelation along the flow direction, $\langle x(0)x(0)\rangle = \frac{k_BT}{k}(1 + W^2/2)$, depends on W, but along the perpendicular direction, $\langle y(t)y(0)\rangle = \frac{k_BT}{k}\exp(-\frac{t}{\tau})$, it does not depend on W [24]. In a quiescent fluid cross-correlations between particle displacements in *orthogonal directions* vanish: $\langle x(t)y(t')\rangle = 0$. But shear flow causes in the shear plane finite cross-correlations [21,23,28], which are asymmetric with respect to $t \to -t$ [24]:

$$\langle x(t)y(0)\rangle = \frac{k_BT}{k}\frac{W}{2}e^{-t/\tau}\left(1 + 2\frac{t}{\tau}\right), \qquad (6)$$

$$\langle x(0)y(t)\rangle = \frac{k_BT}{k}\frac{W}{2}e^{-t/\tau}. \qquad (7)$$

The algebraic prefactor in Eq. (6) illustrates that a fluctuation $y(0) \neq 0$ of a particle is carried away by the flow in the x direction before the initial displacement $y(0)$ relaxes. This leads, during an initial period shorter than the relaxation time τ, to a growth of $\langle x(t)y(0)\rangle$, while the expression in Eq. (7) decays monotonically. As shown in Fig. 2, the predicted elementary signatures for the shear-induced cross-correlations, cf. Eq. (6), are in agreement with our experimental data (triangles). Here $\langle x(t)y(0)\rangle$ takes its maximum roughly at $t \approx 0.009s$, corresponding via Eq. (6) to a particle's relaxation time $\tau \approx 0.018s$. Also the initial decay of $\langle x(0)y(t)\rangle$ (squares in Fig. 2) agrees with our model; cf. Eq. (7). The additionally observed minimum is possibly caused by a slight inclination of the laser beam or it is a reminiscent of a long wavelength oscillation due to the limited number of samples taken [27]. For fluid velocity fluctuations in orthogonal directions in the shear plane a similar signature as in Eq. (6) has been found [19]. According to Eq. (6) and (7) one obtains the normalized ratios of the static cross-correlations: $\langle x(0)y(0)\rangle/\langle y(0)y(0)\rangle = W/2$ and $\langle x(0)y(0)\rangle/\langle x(0)x(0)\rangle = \frac{W/2}{1+W^2/2}$ [24]. From the fits, as indicated by the red and blue line
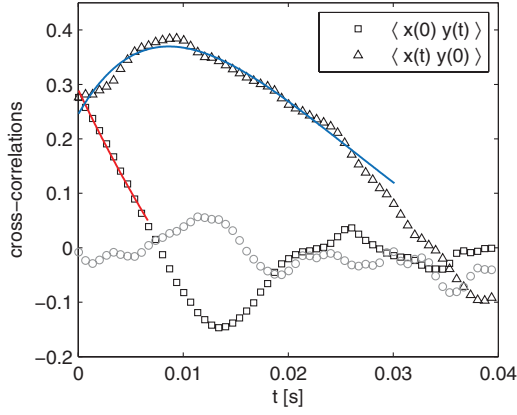
FIG. 2 (color). Shear-induced cross-correlations between orthogonal random displacements: $\langle x(t)y(0)\rangle$ (triangles) and $\langle x(0)y(t)\rangle$ (squares). Lines are fits according to Eq. (6) and (7) and open circles represent $\langle x(0)y(t)\rangle$ in the absence of flow.

in Fig. 2, we obtain $\langle x(0)y(0)\rangle/\langle x(0)x(0)\rangle \approx 0.26$, which corresponds to a Weissenberg number $W \approx 0.62$.

The probability distribution of a Brownian particle in a harmonic potential and exposed to a linear shear flow has an elliptical cross section as shown by the particle's position in Fig. 3 but it has circular symmetry in the absence of flow. The angle ϕ enclosed by the major axis of the particle's probability distribution and the x axis, as well as the ratio R between the lengths of the two principal axes, in the shear plane, depend on the Weissenberg number W as follows [24]:

$$\tan\phi = \tfrac{1}{2}[\sqrt{4 + W^2} - W], \qquad (8)$$

$$R = \left(\frac{\sqrt{4 + W^2} - W}{\sqrt{4 + W^2} + W}\right)^{1/2}. \qquad (9)$$

Using $W \approx 0.62$ as determined above, one obtains via Eq. (8) the angle $\phi \approx 37°$ and via Eq. (9) the ratio $R \approx 0.72$. Within errors this is consistent with the angle $\phi \approx 38°$ and the ratio $R \approx 0.75$ obtained from the measured particle's distribution shown in Fig. 3.

For two particles, each trapped in a potential minimum in shear flow, we investigated the correlations between
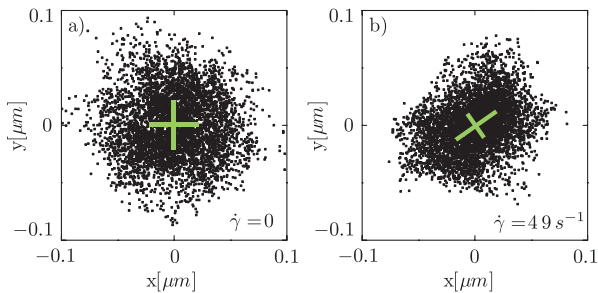

FIG. 3 (color online). The particle's distribution in the shear plane is shown in a) without flow and for a shear flow with $\dot{\gamma} = 49 \text{ s}^{-1}$ in b). The angle between the major and the x axis is $\phi \approx 38°$ and the ratio between the two principal axes is $R \approx 0.75$.

their random displacements for two different configurations: With the connection vector $\mathbf{p}_{12} = \mathbf{p}_1 - \mathbf{p}_2$ parallel to the flow direction as in Fig. 1 or perpendicular to it.

For Brownian displacements of the two distinct particles along the same direction the quantities $\langle x_i(t), x_j(0)\rangle$ and $\langle y_i(t), y_j(0)\rangle$ describe anticorrelations for $i \neq j$ (see, e.g., Ref. [6]). The shear-induced corrections for both are of the order of W^2 as described in more detail in Ref. [24]. For random displacements of distinct particles, but along orthogonal directions, one only finds correlations in the presence of shear flow. With the abbreviations

$$\lambda_{1,3} = 1 \pm 2\mu, \qquad \lambda_{2,4} = 1 \pm \mu, \qquad \mu = \frac{3a}{4d}, \quad (10)$$

and the connection vector $\mathbf{p}_{12}$ parallel to the flow two of the anti-cross-correlations in the shear plane are [24]

$$\langle x_1(t)y_2(0)\rangle = \frac{k_B T}{\mu k} \frac{W}{2}\left(e^{-\lambda_2 t/\tau} + e^{-\lambda_4 t/\tau} - \frac{2\lambda_2 e^{-\lambda_1 t/\tau}}{2 + 3\mu}\right.$$
$$\left. - \frac{2\lambda_4 e^{-\lambda_3 t/\tau}}{2 - 3\mu}\right), \qquad (11)$$

$$\langle x_1(0)y_2(t)\rangle = \frac{k_B T}{k} \frac{W}{2}\left(\frac{e^{-\lambda_2 t/\tau}}{2 + 3\mu} - \frac{e^{-\lambda_4 t/\tau}}{2 - 3\mu}\right). \qquad (12)$$

The cross-correlation $\langle x_1(t)y_2(0)\rangle$ (triangles) in Fig. 4 and the fit (blue line) show a pronounced minimum at about the particles relaxation time $t \approx \tau$.

With a connection vector $\mathbf{p}_{12}$ perpendicular to the flow lines we obtain a cross-correlation $\langle x_2(t)y_1(0)$ in the limit of small values of μ,

$$\langle x_2(t)y_1(0)\rangle \approx -\frac{k_B T}{2k} \frac{W\mu}{2} e^{-t/\tau}\left(3 + 2\frac{t}{\tau} + 6\frac{t^2}{\tau^2}\right),$$

which exhibits in contrast to Eq. (11) two extrema.

Shear-induced cross-correlations between random displacements of a single particle in a potential were calcu-
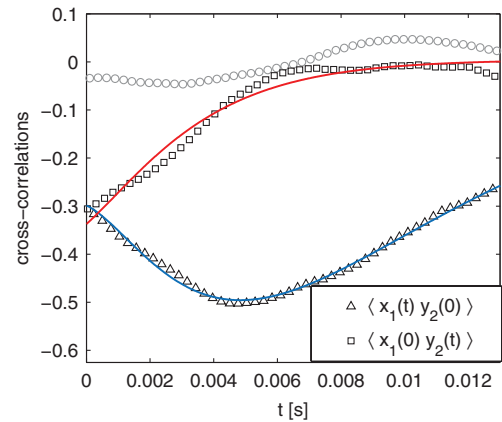

FIG. 4 (color). Correlations $\langle x_1(t)y_2(0)\rangle$ (triangles) and $\langle x_1(0)y_2(t)\rangle$ (squares) between random displacements of two particles. Colored lines are fits according to Eq. (11) and (12). Circles represent the same correlations in the absence of flow.

lated and measured here for the first time, to the best of our knowledge, cf. Fig. 2. At approximately half of the particle's relaxation time τ the correlation function in Eq. (6) exhibits with its maximum a typical signature of Brownian motion in shear flow, caused by the rotational part of the shear flow as well as the non-normal property of the linearized Navier-Stokes equation. Simultaneously, for a particle in a harmonic potential and shear flow an elliptical probability distribution was measured. Both independent measurements are described by a Langevin model for the same value of the Weissenberg number, which confirms the validity of our approach to shear-flow effects on the Brownian particle dynamics.

Theoretically, shear-induced correlations between perpendicular fluid velocity fluctuations have been investigated before [19,20]. Those are traced back to the non-normal property of the linearized Navier-Stokes equation [19] and they are important for the stability of shear flow and the onset of turbulence. The cross-correlations between these velocity fluctuations are based on the same mechanism as discussed here and they exhibit similar extrema as our experimental and analytical results.

Stochastic forces on a suspended particle are caused by velocity fluctuations of the surrounding fluid. Usually, they are assumed to be isotropic in related Langevin models with uncorrelated perpendicular components. However, cross-correlations of the velocity fluctuations in shear flow, as discussed in Refs. [19,20], will modify the cross-correlations between orthogonal particle displacements, as investigated here, but the related additional contributions to the particle displacement correlations are expected to be considerably smaller than the effects of isotropic random forces [24]. It is, however, an interesting and challenging future issue to separate these two nonequilibrium effects in experiments.

For two hydrodynamically interacting particles, each captured by an optical tweezer at the center of the shear flow, we find shear-induced anticorrelations between orthogonal particle displacements with one extremum if the vector connecting the mean particle positions is parallel to the streamlines and two extrema, if the connection vector is perpendicular to the flow lines. These properties may be relevant for further understanding of the dynamics of polymer models in shear flow.

[1] A. Einstein, Ann. Phys. (Leipzig) **17**, 549 (1905).
[2] J. K. G. Dhont, *An Introduction to Dynamics of Colloids* (Elsevier, Amsterdam, 1996).
[3] H. A. Stone and S. Kim, AIChE J. **47**, 1250 (2001).
[4] J. M. Ottino and S. Wiggins, Phil. Trans. R. Soc. A **362**, 923 (2004).
[5] A. Ashkin, J. M. Dziedzic, J. E. Bjorkholm, and S. Chu, Opt. Lett. **11**, 288 (1986); D. G. Grier, Nature (London) **424**, 21 (2003).
[6] J.-C. Meiners and S. R. Quake, Phys. Rev. Lett. **82**, 2211 (1999).
[7] S. Henderson, S. Mitchell, and P. Bartlett, Phys. Rev. Lett. **88**, 088302 (2002).
[8] M. Atakhorrami, G. H. Koenderink, C. F. Schmidt, and F. C. MacKintosh, Phys. Rev. Lett. **95**, 208302 (2005).
[9] J. C. Crocker *et al.*, Phys. Rev. Lett. **85**, 888 (2000).
[10] M. Polin, D. G. Grier, and S. Quake, Phys. Rev. Lett. **96**, 088101 (2006).
[11] P. T. Korda, M. B. Taylor, and D. G. Grier, Phys. Rev. Lett. **89**, 128301 (2002); M. P. MacDonald, G. C. Spalding, and K. Dholakia, Nature (London) **426**, 421 (2003); J. Bammert and W. Zimmermann, Eur. Phys. J. E **28**, 331 (2009).
[12] G. I. Taylor, Proc. R. Soc. A **219**, 186 (1953).
[13] A. Groisman and V. Steinberg, Nature (London) **410**, 905 (2001).
[14] C. Lutz, M. Reichert, H. Stark, and C. Bechinger, Europhys. Lett. **74**, 719 (2006); L. Holzer and W. Zimmermann, Phys. Rev. E **73**, 060801(R) (2006).
[15] T. T. Perkins, D. E. Smith, and S. Chu, Science **276**, 2016 (1997).
[16] P. G. de Gennes, Science **276**, 1999 (1997).
[17] A. Groisman and V. Steinberg, Nature (London) **405**, 53 (2000).
[18] S. Grossmann, Rev. Mod. Phys. **72**, 603 (2000).
[19] B. Eckhardt and R. Pandit, Eur. Phys. J. B **33**, 373 (2003).
[20] G. Khujadze, M. Oberlack, and G. Chagelishvili, Phys. Rev. Lett. **97**, 034501 (2006); A. Jachens, J. Schuhmacher, B. Eckhardt, K. Knobloch, and H. H. Fernholz, J. Fluid Mech. **547**, 55 (2006).
[21] K. Miyazaki and D. Bedeaux, Physica (Amsterdam) **217A**, 53 (1995).
[22] T. B. Liverpool and F. C. MacKintosh, Phys. Rev. Lett. **95**, 208303 (2005).
[23] Y. Drossinos and M. W. Reeks, Phys. Rev. E **71**, 031113 (2005).
[24] L. Holzer, J. Bammert, and W. Zimmermann, arXiv:0911.3264v1.
[25] R. T. Foister and T. G. M. van der Ven, J. Fluid Mech. **96**, 105 (1980); G. G. Fuller, J. M. Rallison, R. L. Schmidt, and L. G. Leal, J. Fluid Mech. **100**, 555 (1980); M. Hoppenbrouwers and W. van de Water, Phys. Fluids **10**, 2128 (1998).
[26] M. K. Cheezum, W. F. Walker, and W. H. Guilford, Biophys. J. **81**, 2378 (2001).
[27] See EPAPS Document No. E-PRLTAO-103-061950 for more details on the experimental setup. For more information on EPAPS, see http://www.aip.org/pubservs/epaps.html.
[28] R. Rzehak and W. Zimmermann, Physica (Amsterdam) **324A**, 495 (2003).